EUROPEAN ORGANIZATION FOR NUCLEAR RESEARCH

CERN/EP 88-177
16 December 1988

Bose-Einstein Correlations for Pions Produced in pp Collisions at 360 GeV/c

NA23, EHS - RCBC COLLABORATION

J. L. Bailly[9], C. Caso[5], Y. Chiba[7d], H. Dibon[12], B. Epp[6], A. Ferrando[8], F. Fontanelli[5], S. N. Ganguli[1], T. Gémesy[2], A. Gurtu[1], R. Hamatsu[7a], P. Hidas[2], T. Hirose[7a], J. Hrubec[12], Yu. Ivanyshenkov[11], T. Kageya[7a], N. Khalatyan[11], E. Kistenev[11], S. Kitamura[7a], V. Kubik[11], J. MacNaughton[12], P. K. Malhotra[1], S. Matsumoto[7c], I. S. Mittra[4], L. Montanet[3], G. Neuhofer[3], G. Pinter[2], P. Porth[12], R. Raghavan[1], T. Rodrigo[8], J. Singh[4], S. Squarcia[5], K. Takahashi[7b], R. Tanaka[7c], L. A. Tikhonova[10], U. Trevisan[5], T. Yamagata[7a], G. Zholobov[11], S. A. Zotkin[10]

[1] Tata Institute of Fundamental Research, 400005 Bombay, India

[2] Central Research Institute for Physics, H-1525 Budapest 114, Hungary

[3] CERN, European Organization for Nuclear Research, CH-1211 Geneva 23, Switzerland

[4] Panjab University, 160014 Chandigarh, India

[5] University of Genova and INFN, I-16146 Genova, Italy

[6] Institut für Experimentalphysik, A-6020 Innsbruck, Austria*

[7a] Tokyo Metropolitan University, Tokyo 158, Japan

[7b] Tokyo University of Agriculture and Technology, Tokyo 184, Japan

[7c] Chuo University, Tokyo 112, Japan

[7d] Hiroshima University, Hiroshima 730, Japan

[8] Centro de Investigaciones Energéticas, Medioambientales y Tecnológicas, E-28040 Madrid, Spain

[9] Université de l'État, Faculté des Sciences, B-7000 Mons, Belgium

[10] Moscow State University, SU-117234 Moscow, USSR

[11] Institute for High Energy Physics, Serpukhov, SU-142284 Protvino, USSR

[12] Institut für Hochenergiephysik, A-1050 Wien, Austria *

Submitted to Zeitschrift für Physik C

* supported in part by Fonds zur Förderung der wissenschaftlichen Forschung

ABSTRACT

Correlations among identically charged pions were measured for pions produced in pp collisions at 360 GeV/c using the EHS spectrometer. The effective radius for pion production was determined to be 1.02±0.20 fm with a chaoticity factor 0.32±0.08. We attempted to obtain the radii in the directions parallel and perpendicular to the beam axis and found no difference between them. No multiplicity dependence of the radius was observed at this energy. A peak near zero in the four momentum transfer distribution showed significant deviation from a single Gaussian. The results of an analysis of the three like pion enhancement were consistent with those for two pions.

1. INTRODUCTION

It is now well known that identically charged pions produced in hadronic processes, as well as in electron-positron annihilations, exhibit interference effects due to Bose-Einstein symmetrization required for the multipion wave function. The effect was first observed in 1960 by Goldhaber, Goldhaber, Lee and Pais [1] in proton-antiproton annihilations and was called the GGLP effect. Later it was realized that the effect was essentially the same as a second order interference phenomenon of photons which was discovered by R. Hanbury Brown and R. Q. Twiss [2] in 1954 and had been used in determining the size of stellar objects.

Goldhaber *et al.*[1] have shown that like-charge pions with small relative momenta are emitted with enhanced probability as compared to an uncorrelated case. If we take the negative of the invariant four momentum transfer squared Q^2, it can be expressed as

$$Q^2 = -(p_1 - p_2)^2 = M_{12}^2 - 4m_\pi^2 \tag{1}$$

where p_1, p_2 are the four momenta of the particle 1, 2, M_{12} is the effective mass of the two particle system and m_π the pion mass. If the pion source is of a Gaussian form $\exp[-(r/\rho)^2/2]$,

then the ratio R of two pion distribution of identical charge pions to an uncorrelated case can be expressed as

$$R(Q^2) = C[1 + \lambda \exp(-\rho^2 Q^2)]. \tag{2}$$

where C is a normalization constant and λ a factor introduced by Deutschmann *et al.* [3] to take care of partial interference. It is often called the chaoticity factor (or the incoherence parameter), since $\lambda = 1$ corresponds to a completely chaotic source for which the Bose-Einstein correlation is maximal.

Kopylov and Podgoretsky [4] used q_T, the component of three momentum difference of two pions $\mathbf{p}_1 - \mathbf{p}_2$ perpendicular to the momentum sum $\mathbf{p}_1 + \mathbf{p}_2$, and q_0 the energy difference $|E_1 - E_2|$. They showed that if the pions come from a radiating spherical surface of radius ρ with incoherent point-like oscillators of lifetime τ, the ratio R will be

$$R(q_T, q_0) = C[1 + \lambda \frac{[2J_1(q_T\rho)/q_T\rho]^2}{(1 + (q_0\tau)^2)}] \tag{3}$$

where J_1 is a first-order Bessel function. A similar expression

$$R(q_T, q_0) = C[1 + \lambda \frac{\exp(-\rho^2 q_T^2)}{(1 + (q_0\tau)^2)}] \tag{4}$$

was derived by G. Cocconi [5] for the case of a Gaussian luminosity distribution. He pointed out the possibility of determining the source size in three dimensions. Several other authors [6- 10] contributed to the sophistication of the theory. Among them, it is to be noted that B. Andersson and W. Hofmann [9] and M. G. Bowler[10] pointed out that the radius ρ obtained did not necessarily represent the actual source length if pions were produced in the way predicted by the string model.

Numerous experiments have been performed to determine the source size using the Bose-Einstein correlation for the hadron-hadron interactions [3][11-18], electron-positron annihilations [19-23] as well as lepton-hadron interactions [24-25] in the energy range from $\sqrt{s}$= 2 to 63 GeV. Their results are summarized in Table 1. Some of the authors used Bessel functions in their analyses, while others preferred a Gaussian form. But the difference of

these two functions is virtually indistinguishable. One should double the ρ values obtained by a Gausssian fit as compared with those obtained with the Bessel functions. Although it was shown that Q^2 is approximately equal to q_T^2 [21], they are not identical. One should note that equations (3) and (4) are not Lorentz invariant, thus their applicability becomes questionable in highly relativistic regions. We prefer to use equation (2) which is Lorentz invariant. Some authors used unlike particle distributions as their reference sample, while others made artificial ones by mixing tracks from different events. Presence of resonances like ρ, ω etc. affects the Q^2 distribution of unlike particles. On the other hand, when making an artificial reference sample, care should be taken in simulating a natural event. Variations in the results presented in Table 1 are partially due to the different methods applied in the analyses.

The situation concerning p-p interactions is somewhat confusing. As is shown in Table 1, the Axial Field Spectrometer Collaboration, using the CERN ISR [14], reported that at $\sqrt{s}$ = 63 GeV for p-p interactions the source size is substantially larger in the direction parallel to the beam axis than in the transverse direction. They showed also that the size is multiplicity dependent, increasing as the number of emitted pions increases. Their findings are contrary to the results obtained for e^+e^- annihilations, where neither directional nor multiplicity dependence of the source size was observed[22][23]. More recently the same Axial Field Spectrometer Collaboration [15] reported that when pions produced in two central jets were selected, no elongation of the source region was observed along the jet axis. ABCDHW Collaboration [17] confirmed the multiplicity dependence of the source size at the highest ISR energy ($\sqrt{s}$ = 63 GeV),but at a lower energy (31 GeV), they found that the multiplicity dependence was very weak. So it is interesting to repeat the same analysis for p-p interactions at comparable energies. Recently the UA1 Collaboration [18] measured the effect for $\bar{p}p$ collisions at $\sqrt{s}$ = 0.2 - 0.9 TeV. They observed the source size roughly independent of energy, but highly dependent on the multiplicity: the higher the multiplicity is, the larger the source size and the smaller the chaoticity factor.

2. DATA SAMPLE

The present analysis was done using the data obtained at a proton beam momentum of 360 GeV/c ($\sqrt{s} = 26$ GeV) by the NA23-experiment performed at the European Hybrid Spectrometer [26]. From an exposure of the hydrogen Rapid Cycling Bubble Chamber [27], a data sample consisting of 9884 events with more than 4 prongs for which all charged tracks were measured, were selected. Pions were identified by ISIS (a multiple sampling drift chamber with a large volume) [28]. For the tracks without ISIS information, those which stopped in the bubble chamber were identified as protons while all other tracks were assigned as pions. In order to restrict the analysis to pions produced in the central region, only those tracks with momenta in the centre-of-mass frame less than 6.5 GeV/c, one half of the maximum possible momentum, were selected. This selection removes high energy protons in the forward direction which may contaminate positive pions. Also tracks with momentum error larger than 4 % were rejected. Checks were made that none of the selections imposed at this level introduce systematic errors on the physical quantities of interest in the subsequent analysis.

3. DATA ANALYSIS

3.1 GLOBAL ANALYSIS

Since it was anticipated that the source size might be multiplicity dependent, the data sample was divided into two groups: one for charged multiplicity less than 13 and the other for the rest. This choice is made in such a way that two samples of equivalent statistical significance are defined: a low and large multiplicity sample, respectively. The Q^2 defined by equation (1) was calculated for all combinations of pions. The Q^2 distribution was obtained by applying weights proportional to the ratio of the number of events to the topological cross section.

A reference sample was formed by combining randomly particles of different events in a data bank of the same multiplicity group. For each event, the sphericity tensor was calculated and the eigenvectors for the tensor were used to define a coordinate system related to the

sphericity axis. All particle momenta were expressed with respect to this system. A hundred thousand random numbers were used to generate data for each multiplicity group, so that sufficient statistics were obtained. The Q^2 distributions of the reference samples for the two multiplicity groups were combined with weights as were done for the real data.

The ratio R of the real data to the reference sample were obtained for all multiplicities (Fig.1) and were compared to the distribution:

$$R(Q^2) = C\frac{1+\lambda\exp(-\rho^2Q^2)}{1+\delta Q^2}. \tag{5}$$

The equation (5) is equivalent to equation (2) with an additional factor δ to take account of the slow variation of R with Q^2 observed beyond the low Q^2 region. In the fitting, the first data points, corresponding to $Q^2 < 0.01$ $(\mathrm{GeV/c})^2$, were always omitted for the reasons described in Section 3.4.

A χ^2-fit of the parameter ρ, λ and δ gave the following results:

$$\rho = 0.99\pm0.17 \text{ fm}, \lambda = 0.37\pm0.08, \delta = 0.09\pm0.14 \ (\mathrm{GeV/c})^{-2} \text{ with } \chi^2(\mathrm{NDF}) = 31(35).$$

Fig. 1 shows the data and the curve corresponding to this fit.

Within the present statistics, the parameter δ is not significantly different from zero. Setting $\delta = 0$ (to recover equation (2)) and using only the data points in the low Q^2 region ($Q^2 < 0.2$ $(\mathrm{GeV/c})^2$), where the Bose-Einstein effect is significant, we obtain

$$\rho = 1.05\pm0.14 \text{ fm}, \lambda = 0.40\pm0.06 \text{ with } \chi^2(\mathrm{NDF}) = 19.6(16),$$

in accordance with the results of the fit which includes the parameter δ.

Our results on ρ and λ are in good agreement with those obtained at similar energies for π^+p and K^+p interactions [12].

To check possible influence of single diffraction dissociation events on ρ and λ, we repeated the analysis for samples where single diffraction dissociation events were eliminated (by introducing a cut on positive tracks: $|X_F| > 0.85$ and a cut on the rapidity gap between the fastest positive track and its neighbour: $\Delta y > 2.5$). We did not observe any significant difference.

3.2 MULTIPLICITY DEPENDENCE

When the ratios R were evaluated and fitted separately for the two multiplicity groups, we obtained for multiplicities less than 13

$\rho = 1.04 \pm 0.22$ fm, $\lambda = 0.36 \pm 0.10$, $\delta = 0.17 \pm 0.15$ $(\mathrm{GeV/c})^{-2}$ with $\chi^2(\mathrm{NDF}) = 31(35)$.

and for multiplicities larger than 13:

$\rho = 0.84 \pm 0.24$ fm, $\lambda = 0.43 \pm 0.13$, $\delta = -0.11 \pm 0.31$ $(\mathrm{GeV/c})^{-2}$ with $\chi^2(\mathrm{NDF}) = 36(35)$.

One does not observe a significant multiplicity dependence, in agreement with the results at $\sqrt{s} = 31$ GeV by the ABCDHW Collaboration [17].

3.3 DIRECTIONAL DEPENDENCE

The four momentum transfer Q^2 may be expressed as

$$Q^2 = Q_T^2 + Q_Z^2 - q_0^2 = Q_T^2 + Q_L^2 \tag{6}$$

where Q_T and Q_Z represent the three momentum transfer components transverse and parallel to the sphericity axis respectively. If one uses the variables Q_T^2 and

$$Q_L^2 = Q_Z^2 - q_0^2, \tag{7}$$

these are invariant to boosts along the jet direction. Dividing our data into a two-dimensional array with 20×20 bins for $0.0 \leq Q_T^2 \leq 0.4$ $(\mathrm{GeV/c})^2$ and $-0.1 \leq Q_L^2 \leq 0.3$ $(\mathrm{GeV/c})^2$ and fitting the function

$$R(Q_T^2, Q_L^2) = C \frac{1 + \lambda \exp(-\rho_T^2 Q_T^2 - \rho_L^2 Q_L^2)}{1 + \delta_1 Q_T^2 + \delta_2 Q_L^2} \tag{8}$$

we obtain:

$\rho_T = 1.23 \pm 0.27$ fm, $\rho_L = 1.10 \pm 0.28$ fm, $\lambda = 0.30 \pm 0.10$,
$\delta_1 = 0.23 \pm 0.10$ $(\mathrm{GeV/c})^{-2}$, $\delta_2 = 0.88 \pm 0.10$ $(\mathrm{GeV/c})^{-2}$ with $\chi^2(NDF) = 397(387)$.

The data together with the curves corresponding to the best fit are shown in Fig.2.

One may conclude that ρ_T and ρ_L are the same within statistical errors. These results are consistent with those found by an ISR experiment [15] but not with [14].

It was observed [29-31] that events of hadron-hadron collisions show remarkable similarities with e^+e^- events at a similar centre-of-mass energy . Especially the sphericity and the thrust distributions were quite similar with those from e^+e^- events, and detailed analysis showed that nondiffractive events were dominantly composed of "di-jet configuration" with the sphericity axis closely aligned with the collision axis.

One might have expected to observe a source size greater in the direction of the sphericity axis of "di-jet" events. But the following argument was presented by Andersson and Hofmann [9] and Bowler[10]. If the string model were correct, then particles produced at the opposite ends of the region will be emitted in opposite directions, and so the length scale measured by Bose-Einstein correlations is hence not the source size, but instead the distance in production points for which the momentum distributions overlap, which should not be very much different in longitudinal or transverse directions.

3.4 Double Gaussian analysis

The Axial Field Spectrometer Collaboration [15] has shown that, analysing their data obtained with ISR in Q rather than in Q^2, the ratio R could be better represented by the sum of two Gausssians,

$$R(Q) = C\frac{1+\lambda_1\exp(-\rho_1^2Q^2)+\lambda_2\exp(-\rho_2^2Q^2)}{1+\delta Q^2} \tag{9}$$

than by a single Gaussian.

We also notice that, when the ratio R is plotted against Q instead of Q^2 as shown in Fig.3, the data deviate significantly from a single Gaussian curve in the region $Q < 0.1$ GeV/c, suggesting that the inclusion of a second Gaussian term would lead to a better fit. The fit to equation (9) produces:

$\rho_1 = 0.97 \pm 0.12$ fm, $\lambda_1 = 0.35 \pm 0.07$,

$\rho_2 = 3.64 \pm 0.85$ fm, $\lambda_2 = 0.85 \pm 0.37$, $\delta = 0.10 \pm 0.03$ $(\mathrm{GeV/c})^{-2}$ with $\chi^2(\mathrm{NDF}) = 30(34)$,

while the fit to a single Gaussian equation gives:

$$\rho = 1.12 \pm 0.12\,\mathrm{fm},\ \lambda = 0.46 \pm 0.07,\ \delta = 0.11 \pm 0.03\ (\mathrm{GeV/c})^{-2} \text{ with } \chi^2(\mathrm{NDF}) = 37(36).$$

Both fits are displayed in Fig. 3. Due to poor statistics we cannot claim that the peak near $Q = 0$ is really a Gaussian. But if it were so, it could be ascribed to resonance effects, since many pions are known to be produced via resonances, which correspond to a larger source size than for direct production. Our findings are consistent with the Axial Field Spectrometer analysis[15]. It is interesting to note that Akhababian et al.[11] observed that the source size measured for negative pions which were decay products of ρ^o was about 3 fm, while those which were not associated with ρ^o gave a source size much smaller.

All our data distributions, expressed either as functions of Q or Q^2, display a peak near $Q = 0$. The statistical errors are too large, however, to attempt systematically to parametrize all the data with a double Gaussian form. Instead, we omitted the first point in Q^2 distribution corresponding to $Q^2 < 0.01$ $(\mathrm{GeV/c})^2$ from the fits. This point was equivalent to the first four points in the Q distribution ($Q < 0.1$ GeV/c) where the strong deviation from a single Gaussian was observed. We estimated the source size of the primary interactions in this way.

3.5 THREE-PARTICLE CORRELATION

The Bose-Einstein enhancement is expected to be even more pronounced for combinations of three or more particles. We have measured three like pion correlations using Q^2 defined as

$$Q^2 = M_{123}^2 - 9m_\pi^2 \tag{10}$$

where the first term represents the square of the invariant mass of the three particles and m_π the pion mass. A reference sample was formed by event mixing technique in the same

way as was done for the two-particle correlation. The distribution thus obtained is shown in Fig.4. Fitting to the equation (5) produced

$$\rho = 0.58\pm0.07\,\text{fm},\ \lambda = 1.19\pm0.22,\ \delta = 0.19\pm0.11\ (\text{GeV/c})^{-2}\ \text{with}\ \chi^2(\text{NDF}) = 21(15).$$

From symmetrization of the wave function for three particles, as compared to that for two particles, it can be shown that ρ for three particles will be $1/\sqrt{3}$ to $1/\sqrt{2}$ of that for two-particle correlation and λ for the former about five times of that for the latter [23]. We found that ρ is about one half of that for two-particle correlation and λ about four times. So what was found is consistent with the two-particle correlation, leaving no space for any additional three-body correlation. The same conclusion was reported by the TASSO Collaboration [23] and the Axial Field Spectrometer Collaboration [15].

3.6 Effect of $\eta'(958)$ decay

Among the many resonances produced, the cascade decays of $\eta'(958)$, $\eta' \rightarrow \pi^+\pi^-\eta$ followed by $\eta \rightarrow \pi^+\pi^-\pi^o$ or $\eta \rightarrow \pi^+\pi^-\gamma$, are known to produce like pions with low Q^2 values. Fig.5 shows the Q^2 distribution for these like pion pairs. One can see that they populate the Q^2 space exactly where the Bose-Einstein correlation effect is maximal. So it is important to estimate the number of η' produced and correct for their effect.

One way of doing this is to use FRITIOF, a Monte Carlo low p_T event generator based on the Lund fragmentation scheme. This model is known to reproduce various aspects of single particle distributions experimentally observed [32]. We processed outputs of the program FRITIOF [version 1.0] with the same criteria as were used in our data analysis and obtained 0.033 like pion pairs per event coming from η' decay. We subtracted them from the Q^2 distribution of our data and repeated the parameter fitting. The result was

$$\rho = 1.06\pm0.23\,\text{fm},\ \lambda = 0.28\pm0.06,\ \delta = 0.10\pm0.11\ (\text{GeV/c})^{-2}\ \text{with}\ \chi^2(\text{NDF}) = 31(35).$$

Since it is not known how correctly resonance production is described in the event generator and since it was pointed out in Ref. [12] that η' production was strongly overestimated, we tried to estimate η' production from our own data.

In a previous paper [33], we used data from the two electromagnetic calorimeters in the EHS spectrometer, for reconstructing particles decaying into two gamma-rays and found that the inclusive η production cross section for $|X_F| > 0.1$ was about 3.5 mb.

Fig.6 shows the M(η,π^+,π^-) effective mass distribution obtained with the present data, using as η the two gamma effective region where an η signal is observed [33]. One can see a small enhancement at the η' mass. The distribution was fitted with a Gaussian centred at 958 MeV, the η' mass, and a smooth background expressed as a polynomial of the third order. The result of the fit is also shown in Fig. 6. It gave 17$\pm$7 η''s of this particular decay mode. Considering the branching ratios of decay modes and correcting for the detector acceptance, we estimated 0.019 like pion pairs per event coming from η' decay, while the FRITIOF event generator predicted 0.033 like pion pairs per event. So a factor of 0.55 was obtained as the ratio of experiment to FRITIOF for the η' production. We used this factor to estimate the amount of data in Q^2 distribution to be subtracted. Fig.7 shows the $R(Q^2)$ distribution after the subtraction. The fitting of the distribution to Eq. (5) gave

$$\rho = 1.02\pm0.20\,\text{fm},\ \lambda = 0.32\pm0.08,\ \delta = 0.10\pm0.12\ (\text{GeV/c})^{-2}\ \text{with}\ \chi^2(\text{NDF}) = 31(35).$$

So we concluded that the correction due to η' is not significant compared to the statistical errors in our analysis.

4. CONCLUSIONS

Table 2 lists all parameters obtained in the present analysis.

We summarize our conclusions as follows:

1) We have observed Bose-Einstein correlations for pions produced in soft p-p interactions at $\sqrt{s} = 26$ GeV.

2) No multiplicity dependence of the source size was observed at this energy.

3) Analysis of its directional dependence indicated a source region with a spherical shape.

4) When the ratio R was plotted against Q, a strong peak near $Q = 0$ was observed. Double Gaussian parametrization yielded a second Gaussian radius of 3.6 fm. This may be ascribed to resonance effects.

5) The effects of $\eta'(958)$ decay were estimated and were found to be negligible at our statistical level.

6) The results of a three-particle correlation analysis were consistent with those of two-particle correlation.

7) Our results are in good agreement with those obtained at similar energies for π^+p and K^+p interactions[12].

ACKNOWLEDGEMENTS

We are deeply indebted to the CERN SPS, beam and EHS crews for their support during preparation and runs of our experiment. Thanks are due to the scanning and measuring staff of our laboratories for their good work which made this analysis possible. We wish to acknowledge with gratitude the support of various funding agencies of the home countries.

REFERENCES

[1]. G. Goldhaber et al., Phys. Rev. **120**, 300(1960)

[2]. R. Hanbury Brown and E. Q. Twiss, Phil. Mag. **45**, 663(1954)

[3]. M. Deutschmann et al., Nucl. Phys. **204B**, 333(1982)

[4]. G. Kopylov and M. Podgoretsky, Sov. Nucl. Phys. **19**, 434(1974); **18**, 656(1973); **16**, 392(1972)

[5]. G. Cocconi, Phys. Lett. **49B**, 459(1974)

[6]. G. N. Fowler and R. M. Weiner, Phys. Lett. **70B**, 201(1977)

[7]. M. Gyulassy, S. K. Kaufmann, and L. W. Wilson, Phys. Rev. **C20**, 2267(1979)

[8]. M. Biyajima, Phys. Lett. **92B**, 193(1982)

[9]. B. Andersson and W. Hofmann, Phys. Lett. **169B**, 364(1986)

[10]. M. G. Bowler, Z. Phys. C - Particles and Fields **29**, 617(1985)

[11]. N. Akhababian et al., Z. Phys. C - Particles and Fields **18**, 97(1983)

[12]. M. Adamus et al., Z. Phys. C - Particles and Fields **37**, 347(1988)

[13]. A. M. Cooper et al., KEK-PREPRINT-79-13 (June 1979)

[14]. T. Åkesson et al., Phys. Lett. **129B**, 269(1983); **187B**, 420(1987)

[15]. T. Åkesson et al., Z. Phys. C - Particles and Fields **36**, 517(1987)

[16]. A. Breakstone et al.,Phys. Lett. **162B**, 400(1985).

[17]. A. Breakstone et al.,Z. Phys. C - Particles and Fields **33**, 333(1987)

[18]. G. Salvini, Talk at XXIV International Conf. on High Energy Phys. Munich(1988)

[19]. G. Goldhaber, Inter. Conf. on High Energy Physics, Lisbon, (Ed. Dias de Deus and J. Soffer) p. 767(1981)

[20]. I. Juričić, Ph. D. Thesis, Univ. of California, Berkeley, LBL-24493, (1987)

[21]. P. Avery et al., Phys. Rev. D **32**, 2294(1985)

[22]. H. Aihara et al., Phys. Rev. D **31**, 996(1985)

[23]. M. Althoff et al., Z. Phys. C - Particles and Fields **29**, 347(1985); **30**, 355(1986)

[24]. M. Arneodo et al., Z. Phys. C - Particles and Fields **32**, 1(1986)

[25]. D. Allasia et al., Z. Phys. C - Particles and Fields **37**, 527(1988)

[26]. M. Aguilar-Benitez et al., Nucl. Instr. and Meth. **205**, 79(1983); Nucl. Instr. and Meth. in Phys. Res. **A258**, 26(1987)

[27]. J. L. Bailly et al., Z. Phys. C - Particles and Fields **23**, 205(1984)

[28]. W. W. M. Allison et al., Nucl. Instr. and Meth. **224**, 396(1984)

[29]. A. Zichichi, Inter. Conf. on High Energy Physics, Lisbon, (Ed. Dias de Deus and J. Soffer) p. 1133(1981)

[30]. D. Brick et al., Z. Phys. C - Particles and Fields **15**, 1(1982)

[31]. J. L. Bailly et al., Phys. Lett. **206B**, 371(1988)

[32]. B. Andersson et al., Nucl. Phys. **B178**, 242(1981)

[33]. J. L. Bailly et al., Z. Phys. C - Particles and Fields **22**, 119(1984)

TABLE 1

Previous experimental results on Bose-Einstein correlation.

Experiment	Reaction	$\sqrt{s}$	Data	Variable	Fitting form	λ	ρ(fm)	Remark
Hadron-hadron Interactions								
Bubble Ch.[3]	$\bar{p}p$	1.88	like/mix	q_T	Eqn.(3)	0.64±0.06	1.45±0.12	*
	π^+p	5.6				0.76±0.02	1.43±0.05	*
	K^-p	5.6				0.75±0.05	1.27±0.08	*
Bubble Ch.[11]	π^-p	8.7	−−/mix	q_T	Eqn.(3)		3.4±0.4	*1
			++/mix				1.2±0.4	*
NA22[12]	π^+p,K^+p	21.7	−−/mix	Q^2	Eqn.(5)	0.35±0.02	0.77±0.03	
			−−/+−			0.38±0.01	0.83±0.02	
Bubble Ch.[13]	pp	28.2	−−/+−	q_T	Eqn.(4)	0.58±0.05	1.50±0.25	*
AFSC[14]	pp	63	like/mix	q_T	Eqn.(3)	λ_T 0.33±0.03	ρ_T 1.8±0.1	*
						λ_Z 0.47±0.07	ρ_Z 3.2±0.3	*
AFSC[15]	pp	63	like/mix	Q_T^2, Q_L^2	Eqn.(8)	0.33±0.03	ρ_T 0.68±0.05	
							ρ_L 0.66±0.05	
ABCDHW[16]	pp	63	like/+−	q_T	Eqn.(4)	0.45±0.03	1.10±0.06	
	$\bar{p}p$	63	like/+−			0.43±0.05	1.05±0.09	
ABCDHW[17]	pp	63,44,31	like/+−	Q^2	Eqn.(5)	0.3–0.5	0.7–1.7	
UA1[18]	$\bar{p}p$	200-900	like/mix	q_T	Eqn.(4)	0.4–0.15	0.7–1.2	
Electron-positron Annihilations								
Mark II[19]	e^+e^-	3.1	++/+−	Q^2	Eqn.(2)	0.71±0.03	0.85±0.02	
Mark II[20]	e^+e^-	3.1	like/+−	Q^2	Eqn.(5)	0.69±0.03	0.77±0.02	
		4–7				0.46±0.04	0.63±0.06	
		29				0.28±0.02	0.75±0.03	
CLEO[21]	e^+e^-	9.46	like/+−	q_T	Eqn.(4)	0.50±0.09	0.99±0.14	
		continuum				0.43±0.07	0.86±0.09	
TPC[22]	e^+e^-	29	like/mix	Q	Eqn.(5)	0.61±0.05	0.65±0.04	
TASSO[23]	e^+e^-	34	like/+−	Q_T^2, Q_L^2	Eqn.(8)	0.31±0.03	ρ_T 0.71±0.11	
							ρ_L 0.72±0.11	
Lepton-hadron Interactions								
EMC[24]	μp	23.4	like/+−	Q^2	Eqn.(5)	0.60–1.08	0.46–0.84	
			or mix					
WA25[25]	νd	SPS wide band ν beam						
			like/+−	q_T	Eqn.(4)	0.48±0.07	0.36±0.04	

In the column of Data, '−−','++' and '+−' mean the combinations of $\pi^-\pi^-$, $\pi^+\pi^+$ and $\pi^+\pi^-$ respectively. 'like' represents a sum of '−−' and '++' combinations. 'mix' stands for an artificial reference sample made up by mixing pions from different events. Subscripts T and Z stand for transverse and longitudinal components of a three-vector, L for difference of longitudinal and time components of a four-vector (see Section 3.3). Those marked with '*' in the column Remark, used a Bessel function J_1. Their ρ values are equivalent to about twice of those obtained with a Gaussian function.

[1] For negative pions, double Gaussian fit gave two radii 1.1±0.5 and 5.5±2.0. The larger radius was attributed to the resonance effect.

TABLE 2

Parameter summary of the present analysis.

Section	Fitting form	ρ fm	λ	δ $(\mathrm{GeV/c})^{-2}$	χ^2(NDF)	Remark
3.1	Eqn.(5)	0.99±0.17	0.37±0.08	0.09±0.14	31(35)	all multiplicities
3.2	Eqn.(5)	1.04±0.22	0.36±0.10	0.17±0.15	31(35)	multiplicities < 13
		0.84±0.24	0.43±0.13	−0.11±0.31	36(35)	multiplicities > 13
3.3	Eqn.(8)	ρ_T 1.23±0.27	0.30±0.10	δ_1 0.23±0.10	397(387)	Q_T^2, Q_L^2 analysis
		ρ_L 1.10±0.28		δ_2 0.88±0.10		
3.4	Eqn.(9)	ρ_1 0.97±0.12	λ_1 0.35±0.07	0.10±0.03	30(34)	Double Gaussian analysis
		ρ_2 3.64±0.85	λ_2 0.85±0.37			
	Eqn.(5)	1.12±0.12	0.46±0.07	0.11±0.03	37(36)	Single Gaussian analysis
3.5	Eqn.(5)	0.58±0.07	1.19±0.22	0.19±0.11	21(15)	Three particle correlation
3.6	Eqn.(5)	1.02±0.20	0.32±0.08	0.10±0.12	31(35)	Final results after correction for η' effect

FIGURE CAPTIONS

Figure 1. $R(Q^2)$ data. The curves are the results of fits to equation (5). In doing the fitting, the first data point was omitted (see text).

Figure 2. $R(Q_T^2, Q_L^2)$ data. The curves are the results of fits to equation (8).

a) Q_L^2 distribution for $0.00 < Q_T^2 < 0.04$ $(\mathrm{GeV/c})^2$.

b) Q_L^2 distribution for $0.04 < Q_T^2 < 0.08$ $(\mathrm{GeV/c})^2$.

c) Q_L^2 distribution for $0.08 < Q_T^2 < 0.12$ $(\mathrm{GeV/c})^2$.

d) Q_T^2 distribution for $-0.03 < Q_L^2 < 0.00$ $(\mathrm{GeV/c})^2$.

e) Q_T^2 distribution for $0.00 < Q_L^2 < 0.03$ $(\mathrm{GeV/c})^2$.

f) Q_T^2 distribution for $0.03 < Q_L^2 < 0.06$ $(\mathrm{GeV/c})^2$.

Figure 3. $R(Q)$ data. The solid curve is the best fit to the double Gaussian equation (9), while the dot-dashed curve is the fit to a single Gaussian equation (5). The dotted and dashed lines correspond to contributions from two sources of different radii in the double Gaussian equation.

Figure 4. $R(Q^2)$ distribution for three like pion combinations. The reference sample was formed by event mixing technique. The curve shows the result of the best fit to equation (5).

Figure 5. Q^2 distribution calculated for like pion pairs produced in the cascade decays $\eta' \rightarrow \pi^+\pi^-\eta$ followed by $\eta \rightarrow \pi^+\pi^-\pi^o$ (solid histogram) or $\eta \rightarrow \pi^+\pi^-\gamma$ (dashed histogram).

Figure 6. The effective mass M(η,π^+,π^-) distribution for $\eta \rightarrow \gamma\gamma$ decay.

Figure 7. $R(Q^2)$ corrected for the effect of η' decays. Data points and the solid line are the results after correction, while the dashed line is the curve before correction.

Fig. 1

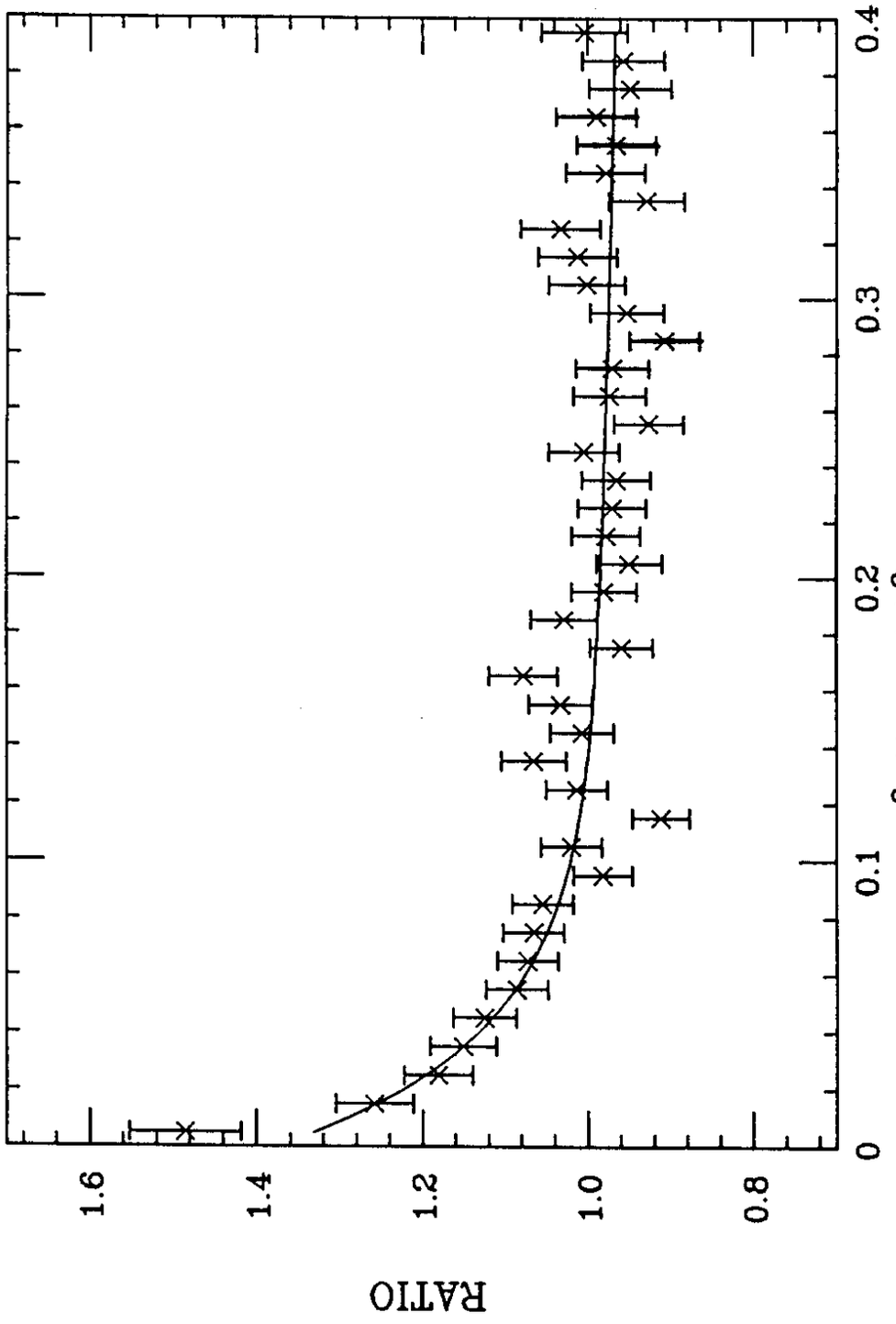

Fig. 2.a

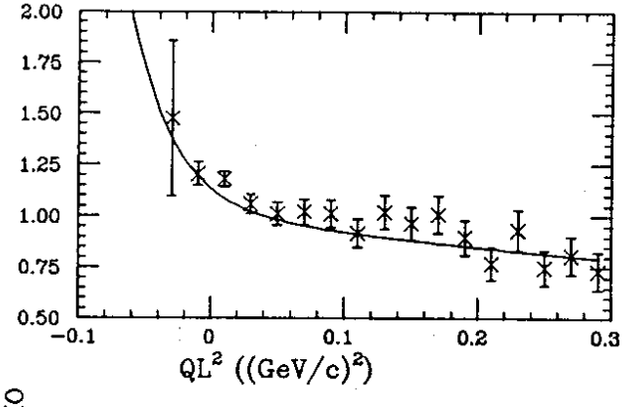

Fig. 2.c

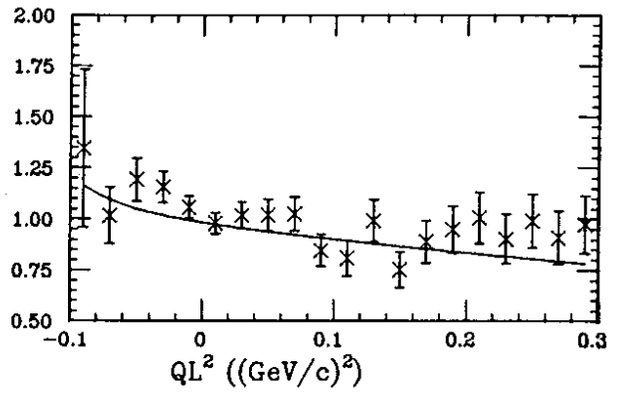

Fig. 2.e

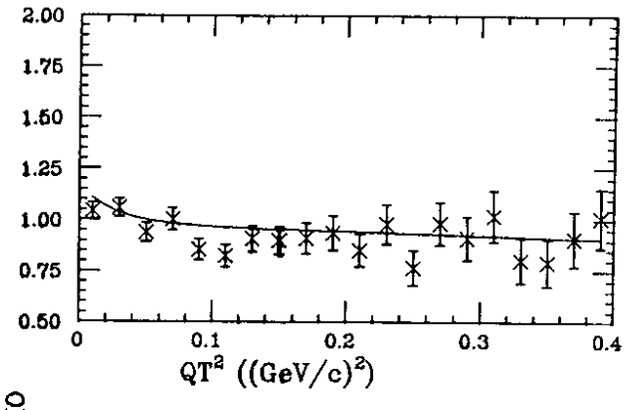

RATIO

Fig. 2.b

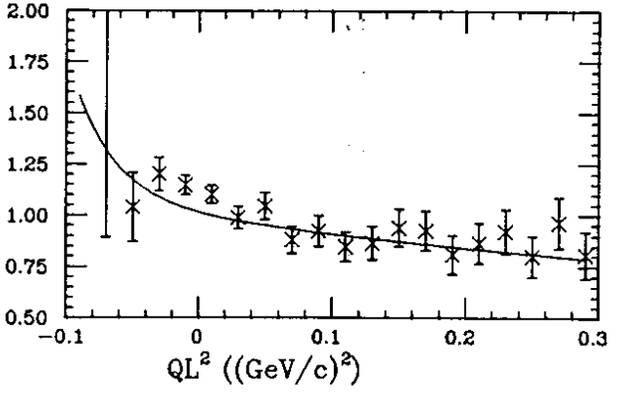

Fig. 2.d

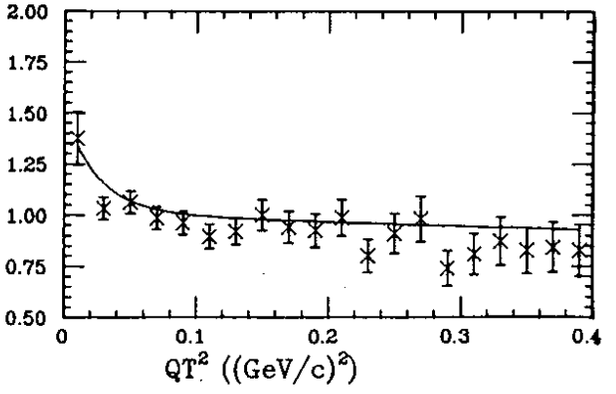

RATIO

Fig. 2.f

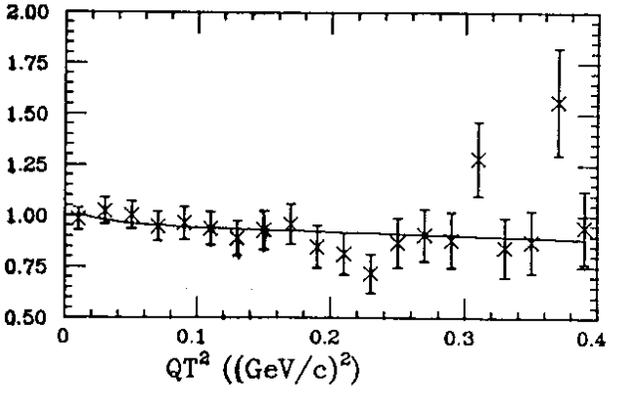

Fig. 3

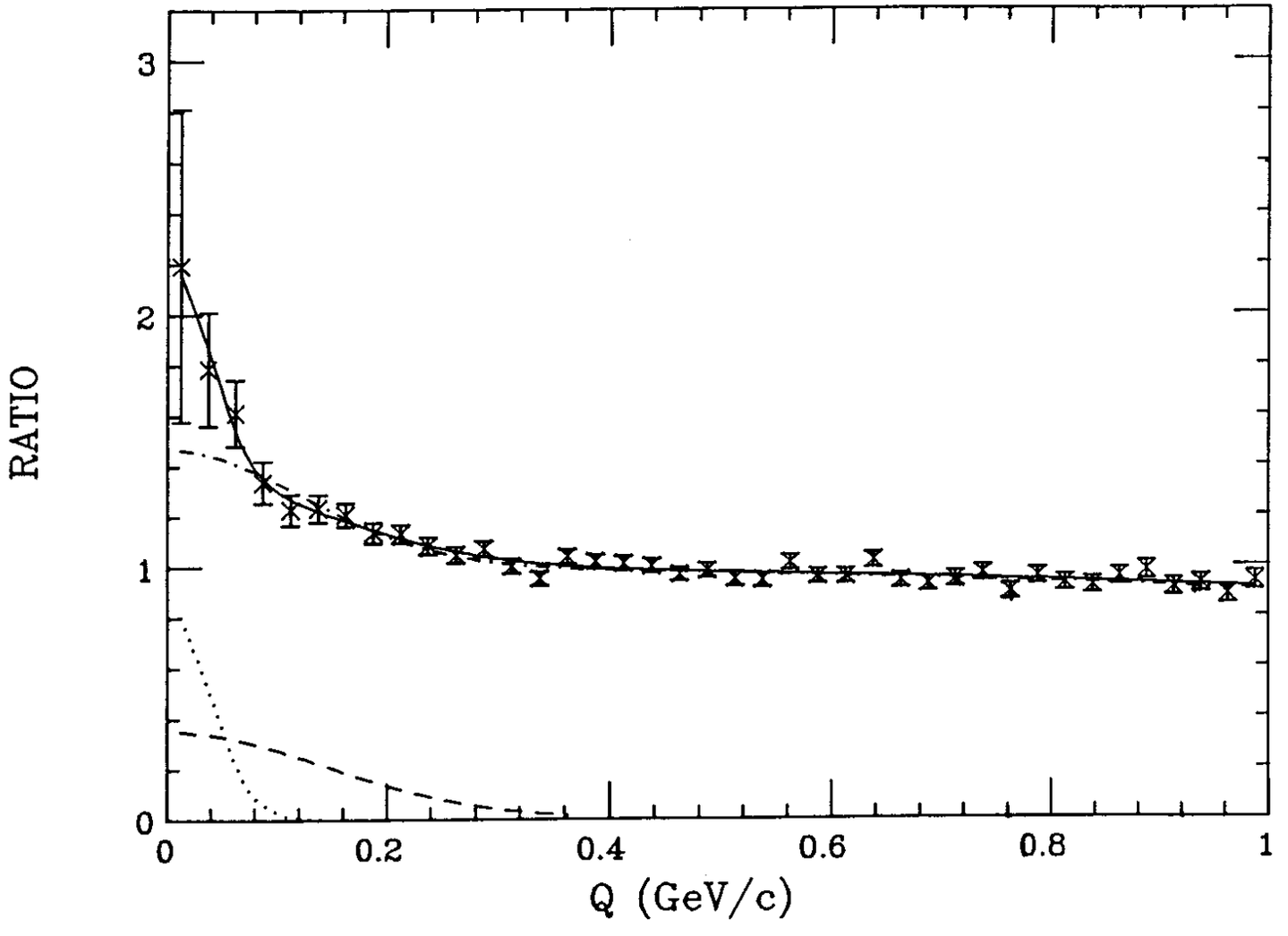

Fig. 4

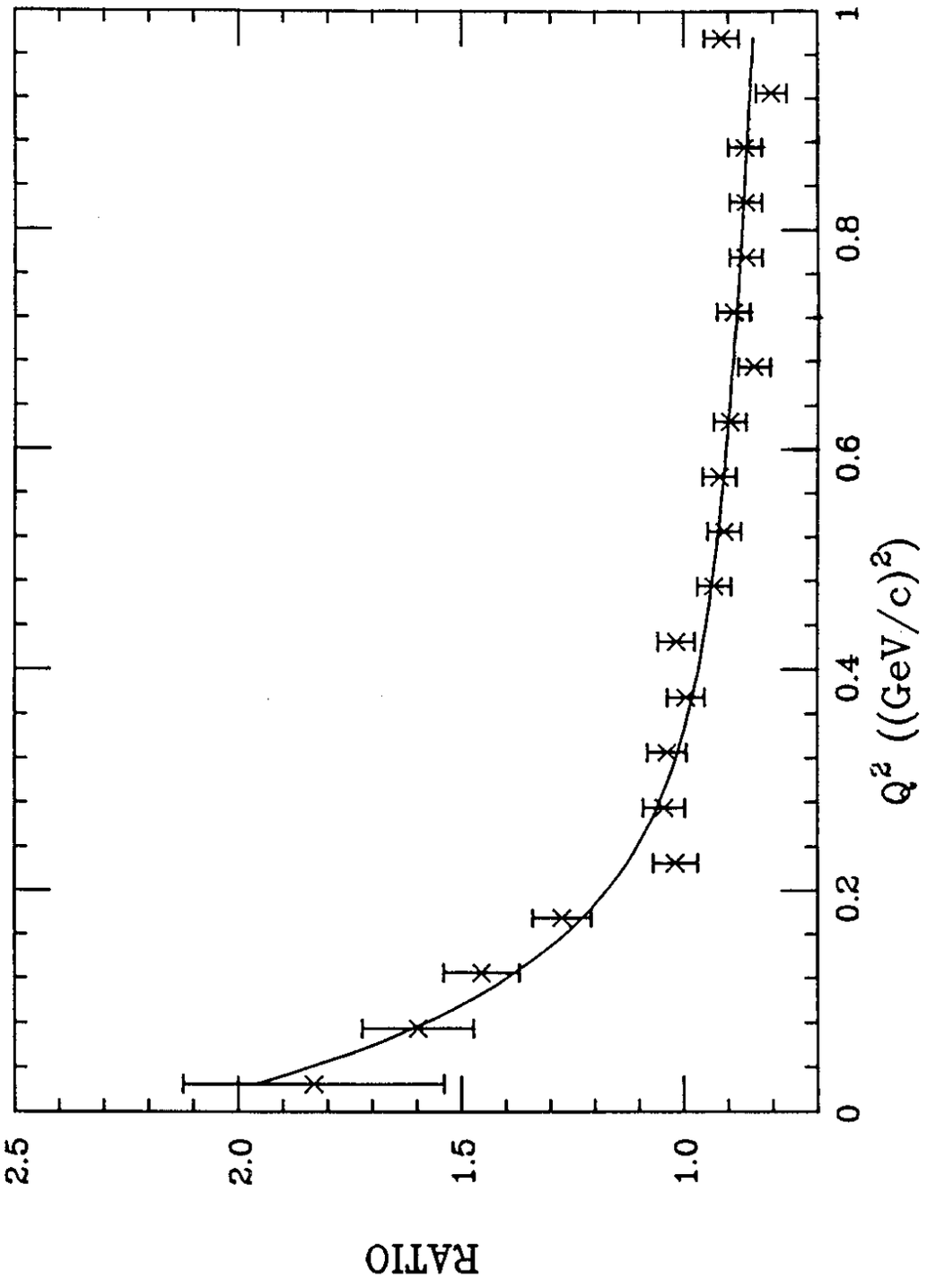

FIG. 5

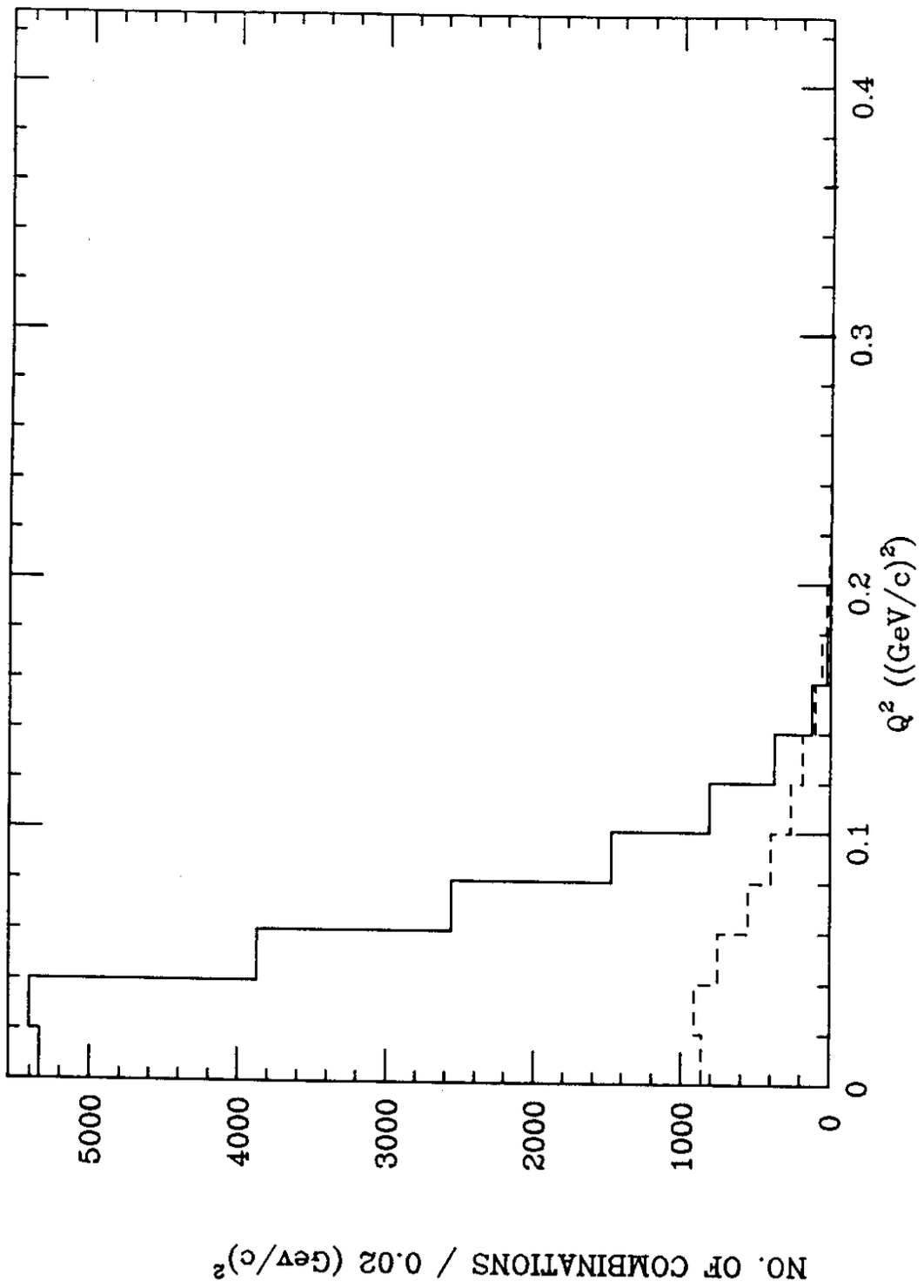
NO. OF COMBINATIONS / 0.02 (GeV/c)²
5000
4000
3000
2000
1000
0
0
0.1
0.2
0.3
0.4
Q² ((GeV/c)²)

FIG. 6

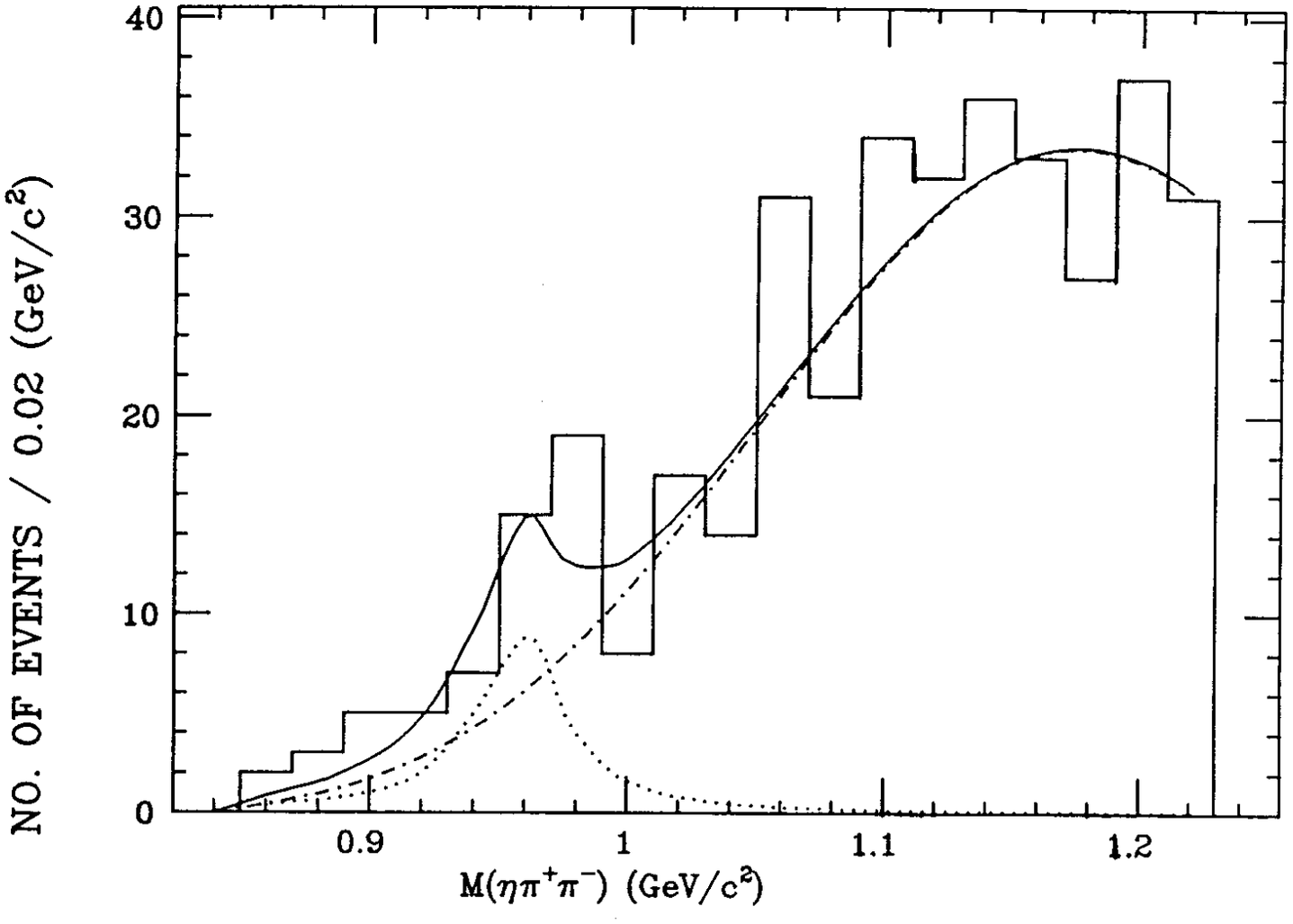

Fig. 7